Accepted Manuscript

Title: Morphological study of polymer surfaces exposed to non-thermal plasma based on contact angle and the use of scaling laws

Author: <ce:author id="aut0005" author-id="S0169433217300363-5f370134b73214c050bd263f4b1647e5"> T. Felix<ce:author id="aut0010" author-id="S0169433217300363-a01334339558ef0cb70fd1eb541928bb"> F.A. Cassini<ce:author id="aut0015" author-id="S0169433217300363-a51de73a4e005d2997d7ed47d55f7dc0"> L.O.B. Benetoli<ce:author id="aut0020" author-id="S0169433217300363-a65891d828278387668f11038f62fadd"> M.E.R. Dotto<ce:author id="aut0025" author-id="S0169433217300363-87e85073e0a59308555f1f5503fde6ca"> N.A. Debacher

PII: S0169-4332(17)30036-3
DOI: http://dx.doi.org/doi:10.1016/j.apsusc.2017.01.036
Reference: APSUSC 34831

To appear in: *APSUSC*

Received date: 22-10-2016
Revised date: 9-12-2016
Accepted date: 5-1-2017

Please cite this article as: T.Felix, F.A.Cassini, L.O.B.Benetoli, M.E.R.Dotto, N.A.Debacher, Morphological study of polymer surfaces exposed to non-thermal plasma based on contact angle and the use of scaling laws, Applied Surface Science http://dx.doi.org/10.1016/j.apsusc.2017.01.036

Short communication: Morphological study of polymer surfaces exposed to non-thermal plasma based on contact angle and the use of scaling laws

T. Felix,* F.A. Cassini,* L.O.B. Benetoli,* M.E.R. Dotto,‡ N.A. Debacher *

*Chemistry Department
‡Physics Department
Federal University of Santa Catarina, Campus Trindade 88040-900- Florianópolis, SC/Brazil.

Graphical abstract

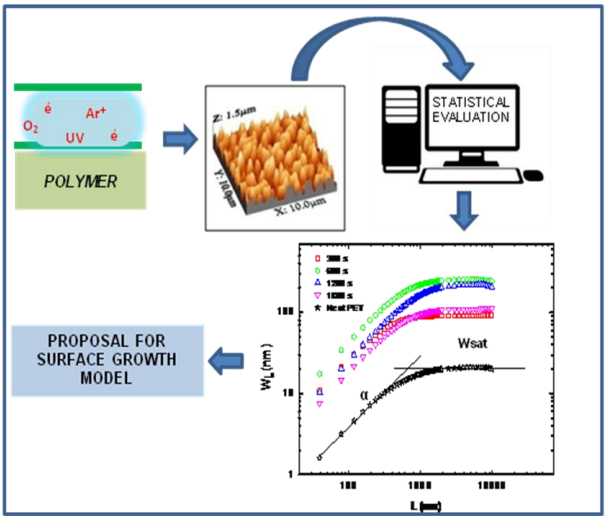

Highlights:

- Polymeric surfaces were etched using non-thermal plasma at different intensities
- Polymers of low mechanical hardness reached the saturation level faster
- A mathematical model based on scaling laws was proposed

ABSTRACT

The experiments presented in this communication have the purpose to elaborate an explanation for the morphological evolution of the growth of polymeric surfaces provided by the treatment of non-thermal plasma. According to the roughness analysis and the model proposed by scaling laws it is possible relate to a predictable or merely random effect. Polyethylene terephthalate (PET) and poly(etherether)ketone (PEEK) samples were exposed to a non-thermal plasma discharge and the resulting surfaces roughness were analyzed based on the measurements from contact angle, scanning electron microscopy and atomic force microscopy coupled with scaling laws analysis which can help to describe and understand the dynamic of formation of a wide variety of rough surfaces. The roughness, R_{RMS} (RMS- Root Mean Square) values for polymer surface range between 19.8nm and 110.9nm. The contact angle and the AFM (Atomic Force Microscopy) measurements as a function of the plasma exposure time were in agreement with both polar and dispersive components according to the surface roughness and also with the morphology evaluated described by Wolf-Villain model, with proximate values of α between $0.91_{(PET)}$ and $0.88_{(PEEK)}$, $\beta = 0.25_{(PET)}$ and $z = 3{,}64_{(PET)}$.

Key words: Polymers, Non-thermal plasma, scaling laws

Short communication

The nature of plasma treatment is well known and involves a series of reactive species, ionized or simply accelerated by an electric field generated between two electrodes [1]. Non equilibrium plasma can be produced under atmospheric or low pressure conditions depending on the desired result and operational capability. Many authors have studied plasma etching in the morphology of metallic and polymeric materials and their effects of cleaning [2] [3], etching and wettability [4] [5], surface energy [6] and energy adhesion [7], [8]. Furthermore, the activation of these surfaces with specific reactants increases the antimicrobial activity or flame retardant capacity [9], [10] among several other properties making the technique of extreme interest. Numerical models that describe plasma systems [11] and the solid-plasma interaction [12]–[17] based on gas flow, density of species, collisional process, etc. [18] are widely reported, and many of these have been used in the development of reactors and optimization processes. Among the methods used to describe the creation of surfaces, the use of the scaling laws has attracted interest [19]–[22] since it contributes to better understanding the chemical structures and the origins of a wide variety of surface roughness profiles. Despite the importance of determining the morphological profiles of polymer surfaces treated by atmospheric non thermal plasmas (NTP) through the scaling laws in order to improve our understanding of how NTP discharge interacts with polymer surfaces, few studies have been published. The scaling properties of a surface roughness represent a very useful tool to investigating understand the growth dynamics of thin films and other deposits [18], [23]. It is well known that a surface can be grown or created using distinct experimental techniques to add or remove materials from the surface, for instance, chemical vapor deposition, spin-casting, chemical etching and sputtering. The morphology generated is a result of the competition between different growth dynamics, and once created the surface can evolve in different ways which will be dependent of many factors, and these are the specific growth parameters. In practice, from plots of the surface width (W) as a function of the matrix size (L) it is possible to obtain the roughness exponent (α) and from plots of the saturation roughness (W_{sat}) as a function of time *t* we can obtain the growth exponent (β). Finally these values are related to some universality class of surface growth [16]. In our work, polyethylene terephthalate (PET) and poly(ether ether)ketone (PEEK) samples were exposed to a non-thermal plasma discharge to different times of exposure, and the resulting surfaces were analyzed based on the contact angle, scanning electron microscopy (SEM) and atomic force microscopy (AFM) analysis. The etched surface with non-thermal plasma discharge images were obtained by AFM, and these

images were treated to evaluate the dynamic, growth, and roughness scaling exponents values using the scaling laws analysis.

The aim of this study was to gain a better understand of the process that controls the formation of the surface using a statistical method based on the scaling laws, where a universality class can help to describe and understanding of the dynamics of the formation of a wide variety of rough surfaces.

Experiments were done with PET donated by Fortymil Plastics (Itatiba, Brazil) and PEEK Vestakeep® (industrial grade) by Evonik Industries (Essen, Germany). These materials were obtained as pellets and molded through simple fusion with a Kapton® (Dupont, USA) film of high heat resistance on a Velp heating plate. The thickness of the films produced was at between 150 and 250 µm. The films were washed with distilled water twice and stored in a dry environment at room temperature. The atmospheric plasma of dielectric barrier discharge (DBD) was generated in a planar geometry made by glass walls and stainless steel electrodes with the following working parameters: argon flow of 5 L/min, gap of 3 mm and pressure of 74.65 kPa. After optimized this parameters, samples were exposed to plasma in the time of 5, 10, 20 and 30 minutes. The power supplied used to generate non-thermal plasma in this work operates at AC mode and at a frequency range from 60 Hz to about 10 kHz. The electrical characteristics of the plasma reactor voltage and current waveforms were investigated using a Teknotronix oscilloscope (model P6015A) couple to voltage (MD03012) and a current (P6022) probes (Florianopolis, Brazil). The electrical parameters adjusted to the experiments were: 2.2 kV and 560 µA at 1W of applied power. By multiplying the current by the voltage (RMS values) measured by the oscilloscope it is possible to estimate the RMS power applied to the NTP reactor. The contact angle and surface energy were determined by depositing three drops of different liquids (water, formamide and diiodomethane) on the surface in a Dataphysics system (model OCA 20) (Filderstadt, Germany) using the ADSA (Axysymmetric Drop Shape Analysis) method. Samples submitted to scanning electron microscopy were coated with gold before analysis on a JEOL microscope (model JSM-6390LV) (Massachusetts, USA). AFM analysis was performed on a Nanosurf FlexAFM Microscope (Massachussets, USA) operating in tapping mode under ambient conditions using a TAP190Al-G tip, scan rate of 1.0 Hz, and the resolution was 512 pixels x 512 pixels. In the same region, a set of images with distinct lateral sizes (areas) was taken, but only the image with 10 μm of lateral size (or 100 μm^2 of area) is shown in this paper. The treatment of AFM images were statistically evaluated using 5.0 WSxM Develp 7.0 software [24]. Then, AFM images were analyzed according to statistical methods of the scaling laws by a mathematical

process using a computer program (C++). The interface width (W_L) was defined by Equation (1). This characterizes the roughness of the interface and it is obtained from the root means square fluctuations of the height as a function of a square matrix of size L [25]:

$$W_L = \sqrt{\frac{1}{L^2}\sum_{i,j}\left(h_{i,j} - \overline{h_L}\right)^2} \quad (1)$$

In equation 1, *h* is the surface height at point (i, j) and the over bar denotes the average values for *h* inside a given matrix of size *L*. The matrix of size *L* scans the whole image under analysis. This is also known as the gliding matrix, where the scanning matrix moves one pixel each step and performs a new spatial average. If the surface presents a self-affine behavior, W_L scales with *L* according to the relation $W_L \sim L^{\alpha}$. The exponent α, which is called the roughness exponent, characterizes the roughness of the saturated interface. As *L* increases, the power-law increases in width, but this will not continue indefinitely, being followed by a saturation regime during which the width reaches a saturation value W_{sat}, which represents a correlation length perpendicular to the surface and scales with time as $W_{sat} \sim t^{\beta}$. β is the growth exponent which characterizes the time-dependent dynamics of the roughening process and, finally, the dynamic exponent (z) shows how the saturation time scales with the sample length and the relationship between the three critical exponents by dividing the roughness by the growth exponent [25].

Figure 1 shows the results for the contact angle and surface energy measurements obtained for the PET (Fig.1(a)) and PEEK (Fig.1(b)) films, respectively. A variation in the contact angle can be clearly observed for the two films. The contact angle value is high for the untreated films and it decreases as a function of the non-thermal plasma exposure time, resulting in an increase in the surface energy and, consequently, an increase in the wettability for both films. After 1800 s of plasma treatment, the contact angle decreases by around 30% compared with its initial value and the surface free energy, related to the polar and dispersive components, increases. These properties are related to two tension components dispersive *d* and polar *p*, according to Equation (2) [14]:

$$\gamma_L(1 + \cos\theta) = 2\left[\left(\gamma_S^d\,\gamma_L^d\right)^{\frac{1}{2}} + \left(\gamma_S^p\,\gamma_L^p\right)^{\frac{1}{2}}\right] \quad (2)$$

where γ is surface tension values related to *S* (solid) and *L* (liquid). An interesting point that can be observed in Fig. 1 is that the polar component increases while a subtle decrease in the value for the dispersive component can be observed. This increase in the polar component can be attributed to the charge accumulation effect and roughness on the surface created during the

plasma treatment [1]. Regarding the accumulation of static electric charges, recent studies show that macromolecules or fragments existent in the original surface, whose dipole moment (*p*) undergoes orientation by the electric field of the plasma discharge, could contribute to the hydrophilic nature conferred to the surface [26]. As can be seen, the surface energy of the samples without treatment is basically related to hydrophobic groups on the surface, but after exposure to the plasma discharge these adopt a hydrophilic character. Figure 1 (b) shows that during the first few minutes of application both the contact angle and surface energy change considerably, reaching a plateau after 1200 s for PEEK. This plateau was not observed for PET even after 1800 s of exposure.

The behavior described in the previous section can be easily observed through the microscopy images obtained from the SEM analysis, shown in Figures 2 (a) and (b). Initially, the surfaces for both materials are homogeneous, apart from a few imperfections arising from the molding treatment to which they were subjected. In the case of PET, during the first five minutes, it was possible to observe the appearance of valleys or paths formed by the plasma discharge. At high magnification it is also possible to detect these formations for PEEK, but at a lower intensity. After 600 s of exposure preferential peaks remain while erosion continues. After 1200 s it can be noted that for PET, exposure to the plasma causes substantial homogeneity and low roughness, features very similar to those observed for the original sample. This behavior is also expected for PEEK however features such as hardness and mechanical strength could be related to the weakness and fragility due to the highly reactive species generated by non-thermal plasma. According to published data, the hardness values for PET and PEEK, determined by the Rockwell method, are 105 and 126, respectively [27].

The AFM images for the PET and PEEK surfaces can be seen in Fig. 3 and they show the morphological surface during exposure. The roughness of surfaces range between 19.8nm and 110.9nm for PET and between 30.5nm and 79.1nm for PEEK. Under the non-thermal plasma treatment, the surface roughness increases up to 900-1200 s for both polymers and then decreases. During surface treatment the plasma reactor parameters were kept constant and there was no change in temperature detected over the treated surface after 1800 s 30 min. Based on the experimental data there is no evidence of thermal effect as expected [1], and it must be related to the mechanical resistance of the materials.

Figure 4 shows W_L as a function of width and the saturation roughness (W_{sat}) as a function of the plasma exposure time, both in log-log plots. We can clearly observe on Fig.4(a) and (b) two regions: slope and saturation regions. From the slope region we obtain the roughness exponent

(α) and from the saturation region we obtain the saturation roughness (Wsat), which is similar to the R_{RMS} roughness. The α values obtained were around 0.91 and 0.88 for PET and PEEK samples, respectively.

The roughness of surface, in this case represented by W_{sat}, was determined according to the plasma exposure time. As mentioned above, despite the slopes of the curves in Figure 4(c), we can obtain the growth exponent (β) which provides information regarding the time evolution of the surface. In the first 10 min of plasma treatment the PET samples present a linear dependence with time, where $\beta \sim 0.25$. In the case of the PEEK samples there was no linear dependence on the plasma exposure time. For samples not exposed to the plasma discharge, the initial roughness values were approximately 21nm and 27nm for PET and PEEK, respectively. When the samples were submitted to plasma, a considerably difference in the roughness values was observed. The PET samples showed an increase in the roughness as the exposure time increased reaching a maximum value of 250nm after 600 s of treatment time, followed by a slight decrease after the longest plasma exposure time. In the case of PEEK samples, there was a slight increase toward a saturation value after longer plasma exposure times. On comparing the roughness for the samples, PET had a higher value than PEEK. This behavior confirms the changes observed in the contact angle in the first minutes of exposure, with an abrupt increase in the roughness of the surface. In order to better understand the formation of polymer surfaces, which in this case occurs due to the erosion of the surface as an effect of the exposure to the NTP discharge, in a chemical-bonding environment some models can be used to describe the growth dynamics of the surface. We can relate the values of the exponents obtained to the linear surface diffusion equation under a chemical-potential gradient, the so-called Wolf-Villain equation (WV), defined in Equation 3, as follows:

$$\frac{\partial h}{\partial t} = R_D - \nu\nabla^4 h + \eta \qquad (3)$$

where R_D is the deposition rate, v is a constant, η is a roughening term with stochastic characteristics of a fluctuation process, and the term $-\nu\nabla^4 h$ represents smoothening by surface diffusion. The values for the roughness, growth and dynamic exponents obtained from this model were 1, 1/4, and 4, respectively. In relation to the values for the roughness exponent obtained with the model and in our results, the experimental α value varies between 0.91 and 0.88, which is lower than the theoretical value of 1. This difference may be related to erosion which could be due to the plasma strength in some regions that contain hard sites which could not be removed

from the surface, referred to in the scaling laws a quenched noise [28] . Although it was not possible to estimate the growth exponent (β) for PEEK, due to saturation behavior, for PET we noted that the value obtained experimentally (0.25) is in agreement with the proposed model and also the dynamic exponent *z* (around 4). Thus, plasma erosion removes species more easily from PET than from PEEK surfaces, probably because PET is a softer polymer than PEEK, as demonstrated by the hardness results [27]. Initially, the plasma etching will attack the easier sites, resulting in a greater degree of roughness of the surface. In agreement with the images obtained by scanning electron and atomic force microscopy, polymeric materials may differ in terms of their mechanical properties and the intensity of damage caused by “heavy” and fast species occurs at different intensities.

ACKNOWLEDGEMENTS

The authors would like to thank LCME-UFSC for technical support with the electron microscopy and LMPT/CTC-UFSC for the contact angle measurements. The authors are also grateful to the Brazilian agency CNPq for financial support.

REFERENCES

[1] A. Fridman, *Plasma Chemistry*. Cambridge University Press, 2008.

[2] C. Rodríguez-Villanueva, N. Encinas, J. Abenojar, and M. A. Martínez, “Assessment of atmospheric plasma treatment cleaning effect on steel surfaces,” *Surf. Coatings Technol.*, vol. 236, pp. 450–456, 2013.

[3] N. Encinas, J. Abenojar, and M. A. Martínez, “Surface & Coatings Technology Extreme durability of wettability changes on polyole fi n surfaces by atmospheric pressure plasma torch,” *Surf. Coat. Technol.*, vol. 205, no. 2, pp. 396–402, 2010.

[4] M. R. Sanchis, V. Blanes, M. Blanes, D. Garcia, and R. Balart, “Surface modification of low density polyethylene (LDPE) film by low pressure O2 plasma treatment,” *Eur. Polym. J.*, vol. 42, no. 7, pp. 1558–1568, 2006.

[5] M. R. Sanchis, O. Calvo, O. Fenollar, D. Garcia, and R. Balart, “Characterization of the surface changes and the aging effects of low-pressure nitrogen plasma treatment in a polyurethane film,” *Polym. Test.*, vol. 27, no. 1, pp. 75–83, 2008.

[6] A. Kamińska, H. Kaczmarek, and J. Kowalonek, “The influence of side groups and polarity of polymers on the kind and effectiveness of their surface modification by air plasma action,” *Eur. Polym. J.*, vol. 38, no. 9, pp. 1915–1919, 2002.

[7] N. Encinas and J. Abenojar, “International Journal of Adhesion & Adhesives Development of improved polypropylene adhesive bonding by abrasion and atmospheric plasma surface modifications,” vol. 33, pp. 1–6, 2012.

[8] X. Jin, W. Wang, C. Xiao, T. Lin, L. Bian, and P. Hauser, “Improvement of coating durability, interfacial adhesion and compressive strength of UHMWPE fiber/epoxy composites through plasma pre-treatment and polypyrrole coating,” *Compos. Sci. Technol.*, vol. 128, pp. 169–175, 2016.

[9] R. Davis, A. El-Shafei, and P. Hauser, “Use of atmospheric pressure plasma to confer durable water repellent functionality and antimicrobial functionality on cotton/polyester blend,” *Surf. Coatings Technol.*, vol. 205, no. 20, pp. 4791–4797, 2011.

[10] B. Edwards, A. El-Shafei, P. Hauser, and P. Malshe, “Towards flame retardant cotton fabrics by atmospheric pressure plasma-induced graft polymerization: Synthesis and application of novel phosphoramidate monomers,” *Surf. Coatings Technol.*, vol. 209, pp. 73–79, 2012.

[11] A. Bogaerts and R. Gijbels, “Numerical modelling of gas discharge plasmas for various applications,” vol. 69, pp. 37–52, 2003.

[12] R. Wang, Y. Shen, C. Zhang, P. Yan, and T. Shao, “Comparison between helium and argon plasma jets on improving the hydrophilic property of PMMA surface,” *Appl. Surf. Sci.*, vol. 367, pp. 401–406, 2016.

[13] G. G. Lister, “Plasma modelling for surface processing,” *Vacuum*, vol. 45, pp. 525–534, 1994.

[14] R. Abd Jelil, X. Zeng, L. Koehl, and A. Perwuelz, “Modeling plasma surface modification of textile fabrics using artificial neural networks,” *Eng. Appl. Artif. Intell.*, vol. 26, no. 8, pp. 1854–1864, 2013.

[15] R. Hrach, S. Novák, and V. Hrachová, “Computational study of plasma-solid interaction at low and medium pressures,” *Vacuum*, vol. 81, no. 6 SPEC. ISS., pp. 774–776, 2007.

[16] J. Zhao, S. Jiang, X. Ji, L. An, and B. Jiang, “Study of the time evolution of the surface morphology of thin asymmetric diblock copolymer films under solvent vapor,” *Polymer*

(Guildf)., vol. 46, no. 17, pp. 6513–6521, 2005.

[17] C. Wang, C. H. Hsu, and I. H. Hwang, “Scaling laws and internal structure for characterizing electrospun poly[(R)-3-hydroxybutyrate] fibers,” *Polymer (Guildf).*, vol. 49, no. 19, pp. 4188–4195, 2008.

[18] M. Dotto and M. Kleinke, “Scaling laws in etched Si surfaces,” *Phys. Rev. B*, vol. 65, no. 24, pp. 1–6, 2002.

[19] F. L. Faita, M. E. R. Dotto, L. G. França, F. C. Cabrera, A. E. Job, and I. H. Bechtold, “Characterization of natural rubber membranes using scaling laws analysis,” *Eur. Polym. J.*, vol. 50, no. C, pp. 249–254, 2014.

[20] M. M. Munir, A. B. Suryamas, F. Iskandar, and K. Okuyama, “Scaling law on particle-to-fiber formation during electrospinning,” *Polymer (Guildf).*, vol. 50, no. 20, pp. 4935–4943, 2009.

[21] R. P. Yadav, M. Kumar, A. K. Mittal, S. Dwivedi, and A. C. Pandey, “On the scaling law analysis of nanodimensional LiF thin film surfaces,” *Mater. Lett.*, vol. 126, pp. 123–125, 2014.

[22] D. Aurongzeb, “Etch front roughening in wrinkly metal,” *Appl. Surf. Sci.*, vol. 253, no. 4, pp. 1717–1721, 2006.

[23] F. B. Assis T.A. , Assis RT.A., Benito R.M. , Losada J.C. , Andrade R.F. , Miranda J.G, Souza N.C., Castilho C.M., Mota F.B., “Effect of the local morphology in the Field emission properties of conducting polymer surfaces,” *Phys. Condens. MatterInstPhys*, vol. 25, 2013.

[24] I. Horcas, R. Fernández, J. M. Gómez-Rodríguez, J. Colchero, J. Gómez-Herrero, and A. M. Baro, “WSXM: A software for scanning probe microscopy and a tool for nanotechnology,” *Rev. Sci. Instrum.*, vol. 78, no. 1, 2007.

[25] H. E. Barabási,A. -L. , Stanley, *Fractal concepts in surface growth*. Cambridge University Press, 1995.

[26] E. Bormashenko, G. Whyman, V. Multanen, E. Shulzinger, and G. Chaniel, “Physical mechanisms of interaction of cold plasma with polymer surfaces,” *J. Colloid Interface Sci.*, vol. 448, pp. 175–179, 2015.

[27] J. E. Mark, *Polymer Data Handbook*. Oxford University Press, 1999.

[28] T. Buldyrev, S.V., Barabási, A. -Caserta,L. F.,Havlin, S., Stanley R. E., Vicsek, “Anomalous interface roughening in porous media: Experiment and model,” *Phys. Rev. A*, vol. 45, 1992.

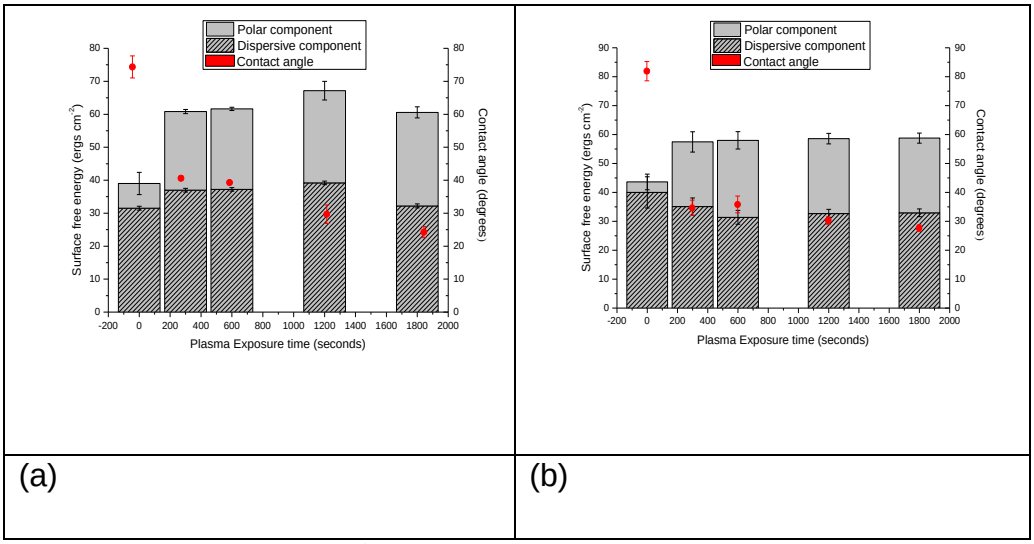

Figure 1: Surface energy (ergs cm^{-2}) and contact angle (degrees) of the (a) PET and (b) PEEK)

(a) PET

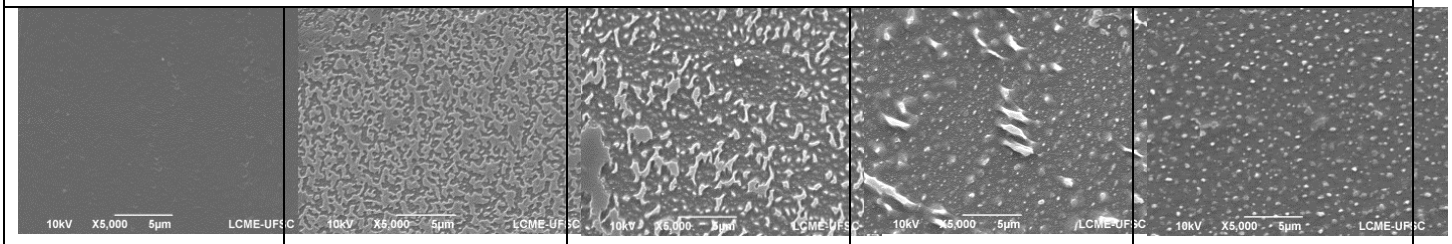

(b) PEEK

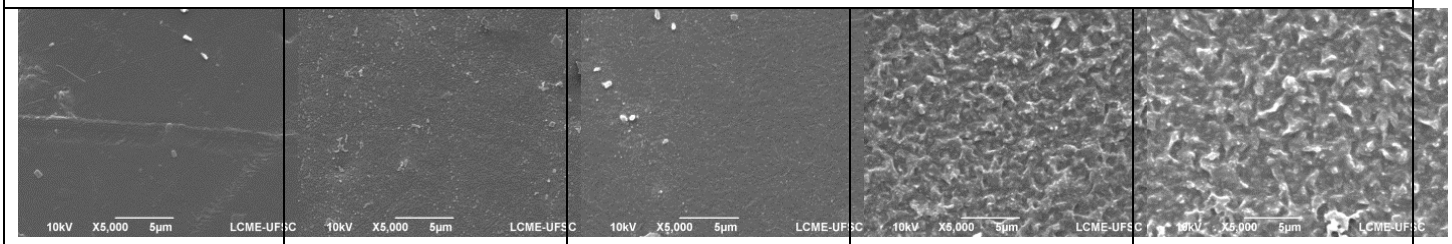

Neat	300 s	600 s	1200 s	1800 s

Figure 2: SEM images of (a) PET) and (b) PEEK as a function of NTP exposure time (argon 5L.min^{-1}; gap 3mm; 74.65kPa).

(a) PET				
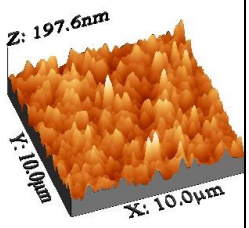	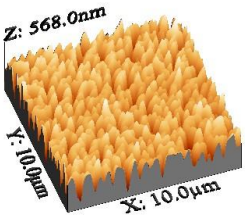	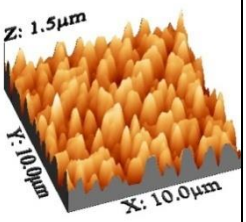	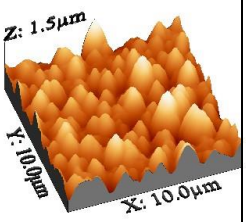	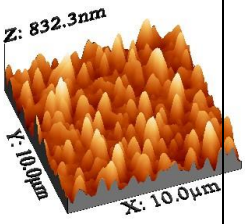
(b) PEEK				
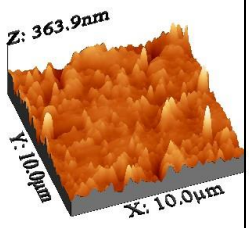	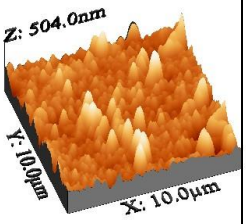	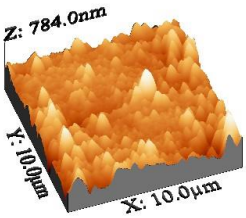	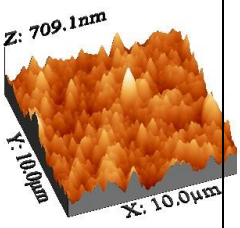	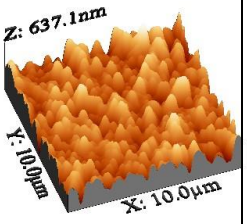
Neat	300 s	600 s	1200 s	1800 s

Figure 3: AFM images for (a) PET) and (b) PEEK as a function of the NTP exposure time (argon 5L.min^{-1}; gap 3mm; 74.65kPa).

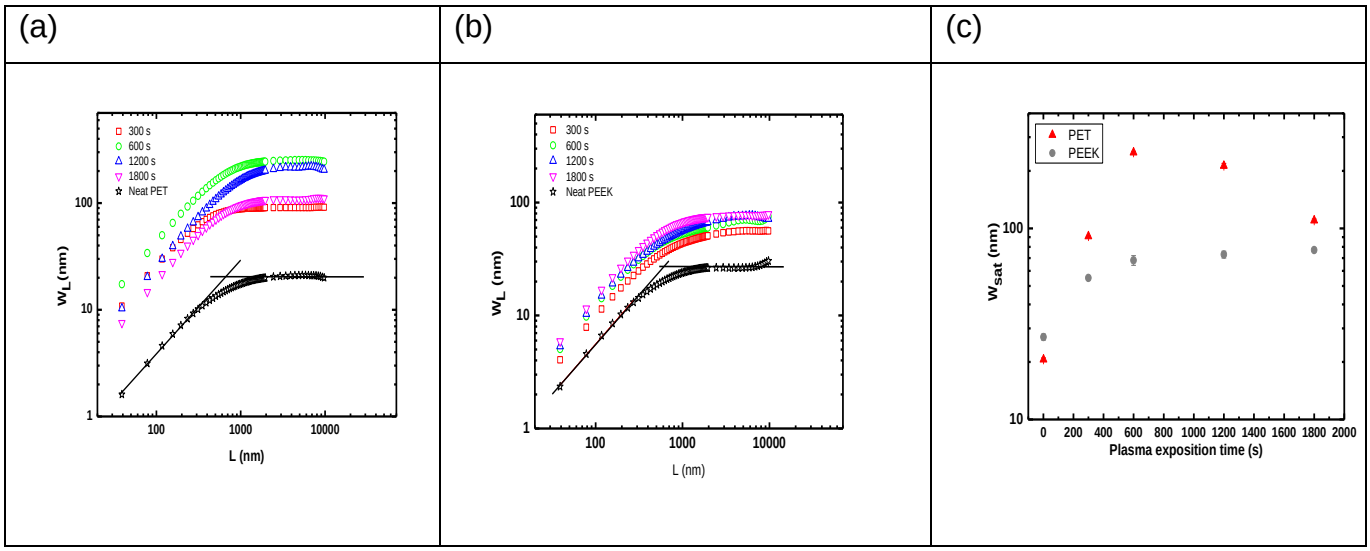

Figure 4: Interface width (W_L) function versus size of matrix L in log-log plots for (a) PET and (b) PEEK and (c) saturation roughness profile (W_{sat}) as a function of plasma exposure time.